

Photon stimulated desorption of hydrogen from diamond surfaces via core-level excitations:  
fundamental processes and applications to surface studies

This article has been downloaded from IOPscience. Please scroll down to see the full text article.

2006 J. Phys.: Condens. Matter 18 S1517

(<http://iopscience.iop.org/0953-8984/18/30/S08>)

View [the table of contents for this issue](#), or go to the [journal homepage](#) for more

Download details:

IP Address: 129.252.86.83

The article was downloaded on 28/05/2010 at 12:28

Please note that [terms and conditions apply](#).

# Photon stimulated desorption of hydrogen from diamond surfaces via core-level excitations: fundamental processes and applications to surface studies

A Hoffman<sup>1</sup> and A Laikhtman<sup>2</sup>

Chemistry Department, Technion—Israel Institute of Technology, Haifa 32000, Israel

E-mail: [choffman@technion.ac.il](mailto:choffman@technion.ac.il)

Received 26 January 2006

Published 14 July 2006

Online at [stacks.iop.org/JPhysCM/18/S1517](http://stacks.iop.org/JPhysCM/18/S1517)

## Abstract

In this paper we review a number of works on photon stimulated ion desorption (PSID) of hydrogen from various diamond surfaces. In particular, we elaborate on the bonding configuration of adsorbed hydrogen (deuterium) and its neighbouring atoms, and its thermal stability in surface and sub-surface regions. Usage of hydrogen PSID as a characterization method involves detailed description of the mechanism and dynamics of hydrogen ion desorption initiated by a synchrotron generated photon beam. Several complimentary analytical techniques (near edge x-ray absorption fine structure spectroscopy, x-ray photoelectron spectroscopy, secondary electron emission measurements) were used to clarify the results of the PSID measurements. The studied systems include hydrogenated/deuterated single-crystal and polycrystalline diamonds, diamond films hydrogenated *ex situ* using microwave hydrogen plasma versus *in situ* hydrogenation by passing hydrogen gas through a hot tungsten filament, hydrogenated diamond films exposed to atomic and molecular oxygen gas, and ion beam damaged diamond films.

## 1. Introduction

Photon-stimulated desorption of ions and neutrals from surfaces is a consequence of primary electronic excitations whose relaxation results in nuclear motion, bond scission and desorption [1, 2]. Desorption induced by core-level excitations may involve direct or indirect electronic processes. Indirect desorption processes are initiated by energetic secondary

<sup>1</sup> Author to whom any correspondence should be addressed.

<sup>2</sup> Present address: Space Environment Section, Soreq Nuclear Research Center, Yavne 81800, Israel.

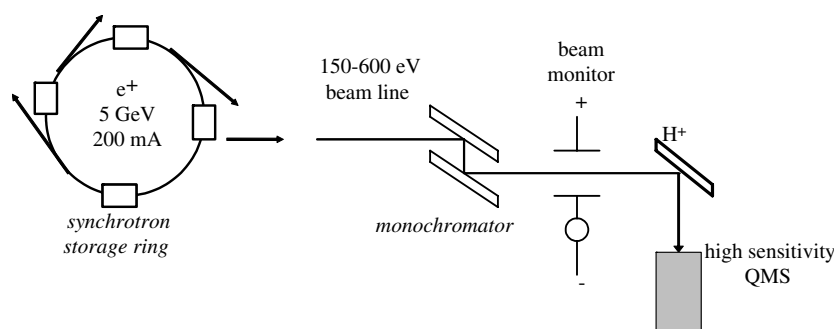


Figure 1. Schematic design of the PSID  $H^+$  experiment.

electrons, which induce valence excitations, whereas direct processes proceed through the relaxation of core holes [3, 4]. Desorption processes stimulated by core-level electronic excitations have been studied extensively in recent years, in particular for the negatively charged desorbing ions [5–11]. Studies of the ion fragments produced by the core-level excitations have yielded insight into dissociation pathways [12–16]. Many of these studies have shown that two-hole, one-electron ( $2h1e$ ) states, in which two holes are produced in the valence band and one electron is excited to an anti-bonding level, are often responsible for ionic dissociation [16].

Desorption of ions from surfaces under photon and electron irradiation, known as photon-stimulated ion desorption (PSID) and electron-stimulated desorption (ESD), respectively, has been recognized as a powerful technique for the investigation of the local electronic structure and bonding of adsorbed species [3]. In both PSID and ESD, the escape probability of ions created below the surface is very small, due to the efficiency of the neutralization process, and therefore ions formed in the surface region are mainly detected. While in ESD mostly  $H^-$  ions are emitted due to valence-band excitations, PSID of  $H^+$  is stimulated by core-level excitations, which are the main objective of this paper.

The study of PSID of hydrogen ions from diamond surfaces is simplified by the fact that these surfaces have a relatively simple electronic structure, composed of one core level and the valence band. In addition, well defined and chemically stable surfaces can be easily prepared. The interaction of hydrogen with diamond surfaces is not only important from the fundamental point of view, but also for many practical applications for which properties mostly affected by surface hydrogen like chemical reactivity and electron emission as well as surface electrical conductivity are considered. However, the determination of adsorbed hydrogen on diamond surfaces is a most difficult experimental problem: commonly used surface sensitive techniques, such as Auger and x-ray photoelectron spectroscopy, are not sensitive to hydrogen. From an analytical perspective, therefore, it is important to determine whether PSID is sensitive to the amount and chemical state of hydrogen adsorbed on diamond surfaces.

## 2. Experimental aspects of PSID measurements

A relatively small number of  $H^+$  PSID measurements of diamond have been reported till now. This is due to experimental difficulties in performing such a work. The C ( $1s$ ) core-level excitation energy of carbon bonded to hydrogen chemisorbed on diamond is 287.5 eV [17] and its presence on the very surface requires utilization of synchrotron radiation as an excitation source with a high sensitivity mass spectrometer to detect the desorbing  $H^+$  ions. The typical experimental set-up is shown in figure 1.

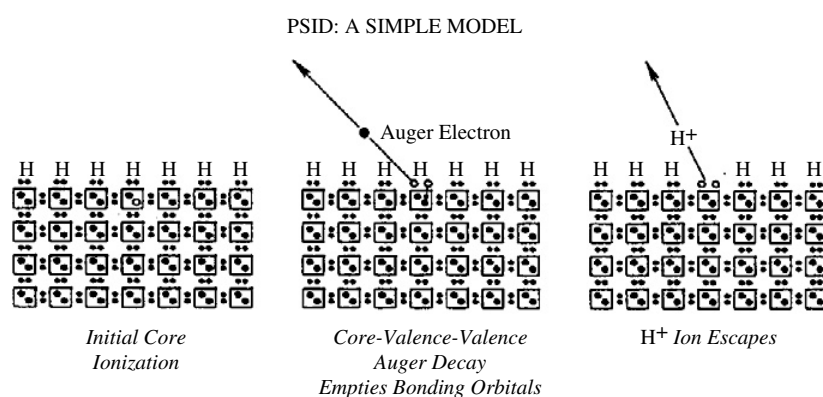


**Figure 2.** Schematics of a KF mechanism for hydrogen photodesorption resulting from an Auger decay (from [20]).

Measuring the kinetic energy distribution of H<sup>+</sup> requires the use of a system equipped with a charged particle (electrons, ions) analyser followed by a mass quadrupole filter for simultaneous mass and kinetic energy analysis. These measurements involve extremely low counting rates and, therefore, require extremely long measuring times and a very intense photon beam [18].

### 3. General mechanism of H<sup>+</sup> PSID desorption from diamond

The first ever study of H<sup>+</sup> PSID from diamond was performed by Pate [19, 20]. The total H<sup>+</sup> ion yield was measured as a function of incident photon energy at and above the carbon K edge (280–350 eV). In spite of the fact that the spectral resolution was quite low, Pate was able to claim that PSID of hydrogen proceeds via a core-level excitation [20], denoted as the Knotek–Feibelman (KF) mechanism [21].

In the case of the diamond–hydrogen system, the KF mechanism would begin with the ionization of the 1s electron on a surface carbon atom (with hydrogen attached)—see figure 2. The resulting KVV Auger transition would leave two holes in the local valence configuration at the surface carbon atom. Should the localized two-hole final state of the Auger transition be sufficiently long lived, a break-up of the carbon–hydrogen bond would follow, resulting in the desorption of H<sup>+</sup> ions. The threshold for such desorption should take place when the incident photon energy increases above the C (1s) C–H bond excitation energy of 287.5 eV [20]. However, there is an alternative desorption process when PSID may result from a direct valence excitation of a bonding electron to an anti-bonding state which results in a dissociation of the surface atom from the bulk [1]. In addition, secondary processes such as photon induced secondary electrons may significantly contribute to the ion desorption yield. In this case both positive and negative hydrogen ions can be desorbed [22]. In the next sections we will discuss the PSID mechanism in more detail.

### 4. PSID from hydrogenated single-crystal and polycrystalline diamond surfaces

PSID H<sup>+</sup> ion yield as a function of incident photon energy from the as-polished natural diamond(111) 1 × 1:H surface, measured by Pate [19], is shown in figure 3. Indeed, there is a large threshold jump in ion yield at the C (1s) excitation energy of 287.5 eV, indicating a core-

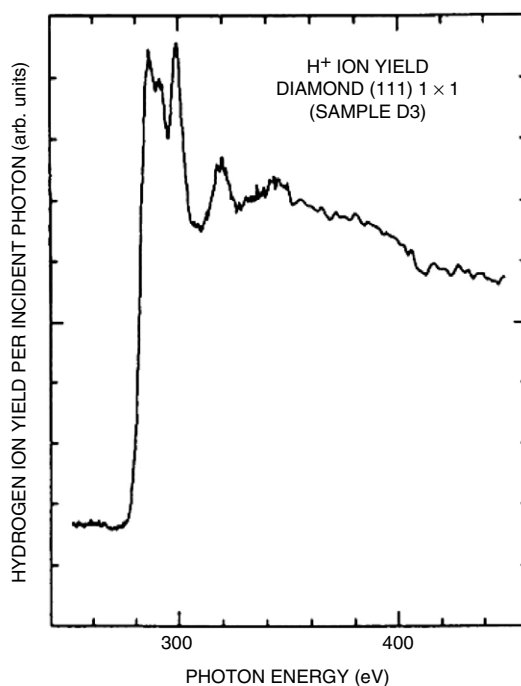


**Figure 3.** PSID  $H^+$  yield from natural (111)-oriented diamond as a function of photon energy (from [19]).

level ionization process. The great importance of these measurements is that they provided the first unambiguous proof of the existence of hydrogen on this type of surface. Moreover, since  $H^+$  ion yield measured following annealing the hydrogenated surface up to  $\sim 950^\circ\text{C}$  was not substantially modified, it was concluded that the hydrogen has a chemisorption bond to the diamond surface.

Annealing the hydrogenated diamond surface above  $950^\circ\text{C}$  resulted in disappearance of the  $H^+$  signal and produced the  $2 \times 2/2 \times 1$  reconstructed surface. Pate also showed that the hydrogenated surface can be restored by *in situ* exposure to hydrogen gas in the presence of a tungsten filament at a temperature of  $1800^\circ\text{C}$ .

After the pioneering work of Pate [19], no further studies of  $H^+$  PSID from diamond were performed for more than a decade until Hoffman *et al* recommenced this type of experiments on both single-crystal and polycrystalline diamond samples [23]. The single-crystal diamond was hydrogenated by microwave (MW) hydrogen plasma, while the polycrystalline films were prepared by MW chemical vapour deposition (CVD). The conditions of both processes were reported elsewhere [18]. The measurements were performed using synchrotron radiation (produced in the 800 MeV SUPER-ACO storage ring located in LURE, Orsay, France) in the range of 150–900 eV. The set-up used in these experiments, entirely different from that of Pate, enabled significantly higher resolution and sensitivity. The photon beam passed through a 9 m plane grating monochromator which provided the energy resolution of better than 0.15 eV. The energy of the emitted secondary electrons was measured by CLAM-2 electrostatic hemispherical energy analyser and, since the analyser and the sample had a common ground, the measured electron kinetic energy is with respect to the Fermi level of diamond. Ions desorbed by this high intensity photon beam were detected by a high resolution quadrupole

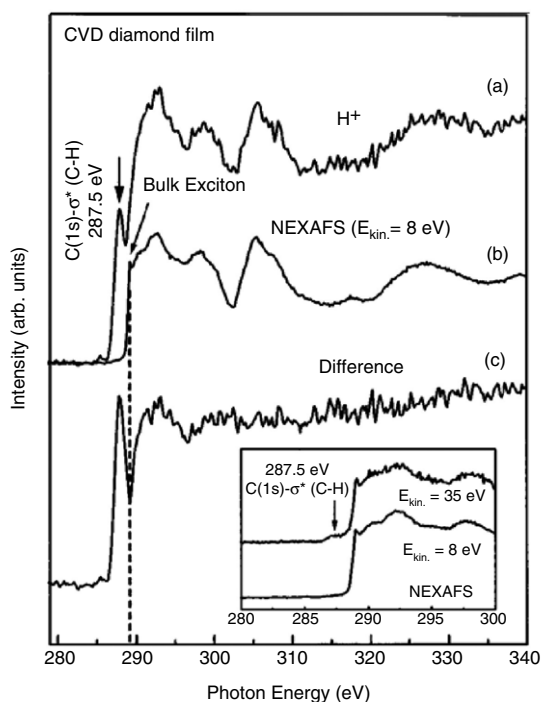


**Figure 4.**  $H^+$  desorption yield from the CVD diamond film as a function of incident photon energy (curve a) compared to the NEXAFS spectrum recorded using 8 eV secondary electrons (curve b). Curve c is the difference between the  $H^+$  yield and the normalized NEXAFS spectrum. In the inset the NEXAFS spectra measured by 8 and 35 eV secondary electrons (bulk and surface sensitive modes, respectively) are shown in the 280–300 eV photon energy range (from [18]).

mass spectrometer (Riber SQX 156), which is not able, however, to determine their kinetic energy. The energy distribution of the  $H^+$  ions was measured using an additional accessory consisting of a cylindrical mirror analyser followed by a mass quadrupole filter for simultaneous mass and kinetic energy analysis. To better explain the PSID results on the basis of surface electronic structure, partial electron yield (PEY) near edge x-ray absorption fine structure (NEXAFS) spectra were measured in the same vacuum chamber by using primary energies near the core level ionization energy of carbon, 280–340 eV and detecting secondary electrons of 8 eV (more bulk sensitive mode) and 35 eV (surface sensitive mode). In such a way the chemical bonding in the near surface region of diamond samples was studied.

The results of  $H^+$  measurements are shown in figure 4 along with the PEY NEXAFS spectrum of 8 eV secondary electrons [18]. The  $H^+$  desorption yield displays features similar to those of the NEXAFS although they seem to be superimposed on a monotonically increasing background except a sharp structure at 287.5 eV, 2 eV lower than the threshold of the NEXAFS spectrum. As similar features were observed in PSID and NEXAFS, the authors subtracted the normalized NEXAFS spectrum from the normalized  $H^+$  yield [18]. The energy scale and the intensity of each spectrum were normalized to the intensity and position of the second bandgap of diamond at 302.4 eV. From the subtracted spectrum it was concluded that the  $H^+$  yield consists of a signal proportional to the total electron yield (TEY) and with a threshold at  $\sim 289$  eV, superimposed to a resonance at 287.5 eV and a signal that varies monotonically with the excitation energy. It appears from that result that the  $H^+$  desorption involves two distinct

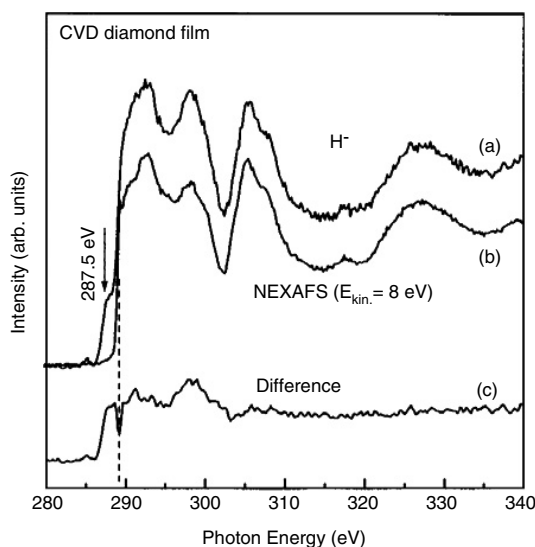


**Figure 5.**  $\text{H}^-$  desorption yield from the CVD diamond film as a function of incident photon energy (curve a) compared to the NEXAFS spectrum measured using 8 eV secondary electrons (curve b). Curve c is the difference between the  $\text{H}^-$  yield and the normalized NEXAFS spectrum (from [18]).

processes: the first  $\text{H}^+$  desorption process is generated by the bulk excitations, i.e., by the large flow of secondary electrons from the relaxation of C (1s) core holes from the bulk carbon atoms. The second process, quite distinct from the first one, is characterized by the resonance at 287.5 eV and does not show the features of the TEY. This may be an indication that the second process is generated by some surface excitations on the diamond film.

Figure 5(a) shows the negative hydrogen ion desorption yield measured in the 280–340 eV range from the CVD diamond film. The  $\text{H}^-$  yield is much more intense than the  $\text{H}^+$  desorption yield. However, an absolute comparison between the  $\text{H}^+$  and  $\text{H}^-$  ion yield intensities is not possible, as the relative sensitivity of the mass spectrometer to the positive and negative hydrogen ions is not known. Following the same procedure as that used for the  $\text{H}^+$  ion yield, the difference between the normalized  $\text{H}^-$  yield and the NEXAFS spectrum was determined (see figure 4(b)). To a great extent the  $\text{H}^-$  yield is proportional to the TEY, which means that the  $\text{H}^-$  photodesorption process is predominantly an indirect process. However, an additional five times less intense contribution is also observed. It includes the same resonance at 287.5 eV as the  $\text{H}^+$  yield, followed by a rather monotonic signal and a broad resonance at  $\sim 298$  eV, which does not appear in the  $\text{H}^+$  yield.

The PSID of  $\text{H}^+$  and  $\text{H}^-$  ions from polycrystalline CVD diamond films are compared in figure 6 to that from the hydrogenated diamond(100) single-crystal sample. From this figure the same features appear in the PSID of  $\text{H}^-$  and  $\text{H}^+$  from both surfaces, but with somewhat different relative intensities. The relative contribution of the direct process is higher in the case of the CVD diamond film than in the case of natural diamond(100) (i.e., the relative intensity of the peak at 287.5 eV of  $\text{H}^+$  yield is higher for the diamond film than for the hydrogenated diamond(100) surface). These small differences may reflect the higher concentration of hydrogen atoms which may be present at boundaries in CVD diamond films. However, other effects may be responsible for this small difference, for example, the angular distribution of the desorbed ions from the diamond(100) surface should peak along bond directions and perhaps the mass spectrometer samples certain directions more efficiently than others.

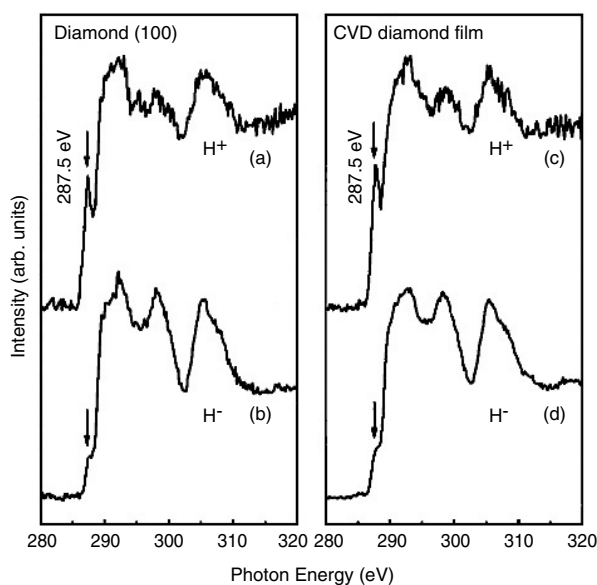


**Figure 6.**  $H^+$  and  $H^-$  yields as a function of the photon energy for diamond(100) (curves a and b) and the CVD diamond film (curves c and d) (from [18]).

It is known that the diamond CVD surface is fully saturated by chemisorbed hydrogen, while some estimate that the bulk hydrogen concentration is less than 1 at.% [16]. In order to verify that the measured  $H^+$  and  $H^-$  PSID reflects a surface process, *in situ* deuteration of the surface was performed and the  $D^+$  and  $D^-$  PSID yields were measured. Following the deuteration process, a  $D^+$  (and  $D^-$ ) signal could be measured when the diamond surface was subjected to photon irradiation, showing that the exchange reaction took place (figure 7). The  $D^+$  ( $D^-$ ) yield as a function of photon energy was similar to that obtained for  $H^+$  ( $H^-$ ), although with much lower intensity. The similarity between the  $H^+$  ( $H^-$ ) and  $D^+$  ( $D^-$ ) yields and photon energy indicates that the photon stimulated  $H^+$  and  $H^-$  desorption yields as a function of photon energy represent a surface process. The differences between the PSID of surface and sub-surface hydrogen (deuterium) will be elaborated in more detail in the next section.

In order to gain some more insight into the PSID process, the authors also recorded the kinetic energy distribution of  $H^+$  ions. These measurements involve extremely low counting rates and, therefore, required long measuring times and a very intense photon beam. The kinetic-energy distribution of photodesorbed  $H^+$  ions from the diamond film was measured for incident photon energies of 290 and 350 eV. A similar distribution was obtained for both photon energies and it is shown in figure 8 for the case where the diamond surface was irradiated by 350 eV photons.

As seen from figure 8, the kinetic energy distribution of  $H^+$  consists of two peaks at 1.7 and 4.0 eV. It was suggested that the sources of the two peaks in the  $H^+$  energy distribution might be the direct and indirect electronic processes responsible for the PSID. The existence of low (1.7 eV) and rapid (4.0 eV) desorbing  $H^+$  ions may be ascribed to one or several of the following effects. First, one could argue that the direct process gives rise to rapid desorbing ions whereas the indirect one gives rise to slow ions. Indeed, the direct process involves a C (1s) hole formation followed by an Auger relaxation. This is expected to result in highly



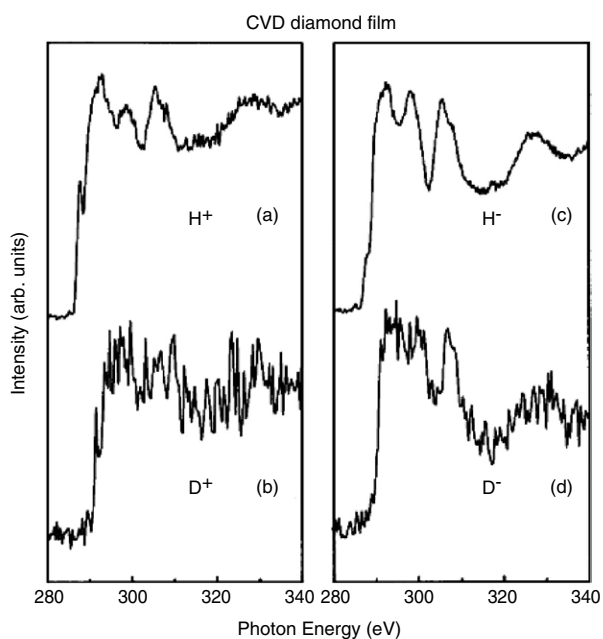


**Figure 7.** H<sup>+</sup> and H<sup>-</sup> desorption yields as a function of incident photon energy (curves a and b) from the hydrogenated CVD diamond film. D<sup>+</sup> and D<sup>-</sup> desorption yields (curves c and d) from the deuterated diamond surface as a function of incident photon energy (from [18]).

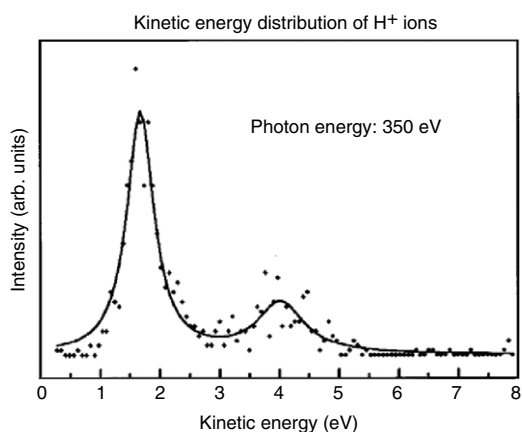


**Figure 8.** Kinetic energy distribution of H<sup>+</sup> photodesorbed ions from the diamond film for a photon excitation energy of 350 eV (from [18]).

ionized species, which may release a high amount of kinetic energy for desorbing ions. In contrast, the indirect process involves only valence electronic excitation, which is expected to release less kinetic energy. Second, one could argue that slow and rapid H<sup>+</sup> ions originate from different adsorption sites. Third, one cannot exclude that for a given H adsorption site and given desorption process (for example the direct process) both slow and rapid H<sup>+</sup> ions can be desorbed due to electronic relaxation of the initially excited state towards two separate repulsive curves.

The study of Hoffman *et al* enabled us to elaborate the PSID desorption mechanism in more details. It revealed two distinct processes for the  $H^+$  and  $H^-$  PSID: the first one results from the surface excitations and the second one from the bulk initiated excitations. The first process is considered to be of a direct nature whereas the second is an indirect one. The second process implies the role of secondary electrons from the bulk of diamond, i.e. indirect processes, for nearly all the  $H^-$  yield and some of the  $H^+$  yield. In this case, two PSID mechanisms may be assumed. The first one involves valence excitations of the hydrogenated surface induced by secondary electrons. Considering that the minimum energy to desorb an  $H^+$  ion may be estimated by the sum of the C–H bond energy (4.3 eV), plus the ionization energy of H (13.6 eV), minus the electron affinity of the hydrogenated diamond surface ( $-0.5$  to  $-1$  eV), this makes a minimum energy to desorb  $H^+$ , which should be around 18–19 eV. Clearly a single valence-band excitation is not likely to be energetic enough to produce ion desorption. As was proposed by Hellner *et al* [24], the excitation to desorb  $H^+$  should involve a multielectron valence excitation, for example ionic satellite state excitations. Secondary electrons with such high kinetic energies (19–50 eV) do exist, as can be seen from the NEXAFS spectrum with electrons having kinetic energies of 35 eV (figure 4). However, these secondary electrons come from the top layers of the diamond sample rather than from the bulk.

$H^-$  desorption may also involve the electron attachment to the hydrogen atoms ejected by a direct process at the surface. It was not possible to measure the yield of atomic hydrogen as a function of the incident photon energy in order to prove that assumption. However, it is known that desorbing H atoms or positive ions may efficiently capture electrons when leaving the surface, giving rise to  $H^-$  photodesorbed ions. The negative electron affinity (NEA) of diamond [25], which results in the photoemission of electrons with very low kinetic energy, would certainly enhance the probability of the electron attachment process.

Turning now to the direct process in the PSID, it should be noted that this process was observed mainly in the  $H^+$  photodesorption yield but also, with reduced probability, in the  $H^-$  yield. It is characterized by a resonance at 287.5 eV, which is 2.0 eV lower than the threshold of the TEY. The energy position of that resonance is the same as the resonance in the surface sensitive NEXAFS where it was associated with a C (1s)– $\sigma^*$  (C–H) transition [26]. Therefore, the resonance at 287.5 eV may be associated with the  $H^+$  photodesorption following the core-level excitation of surface carbon atoms bonded to hydrogen atoms, H(ads). The following mechanism was suggested for this process. After the ionization of the C (1s) level, relaxation of the core hole occurs on a timescale of  $10^{-16}$ – $10^{-17}$  s, characteristic of the electronic processes (see [3] and references therein). This electronic relaxation is much faster than any nuclear motion, responsible for desorption of  $H^+$  that occurs on a timescale of  $10^{-13}$ – $10^{-12}$  s [3]. Obviously, the relaxation of the C (1s) core hole takes place through a downward electronic transition involving the local valence band. It may result in a radiative (emission of x-rays) or a nonradiative transition, involving the emission of a third electron (Auger electron) as a mean to relax the excess electron energy. For the low  $Z$  elements, such as carbon, a nonradiative or Auger type relaxation process is preferred with a probability of nearly unity. Therefore, the most probable relaxation process of the C (1s) core hole is through an Auger transition leading to the emission of a C (KLL) Auger electron with  $\sim 270$  eV kinetic energy and formation of two localized valence-band holes. When the ionization occurs in a carbon atom bonded to a hydrogen atom, the localized two-hole states in the C–H(ads) bond may cause the bond breaking and the emission of  $H^+$  through the charge separation as the most likely way to relax the large hole–hole repulsive interaction. This process may explain desorption of  $H^+$  ions, but cannot account for desorption of negative species, such as  $H^-$ .

The contribution of the resonance at 287.5 eV to the photodesorption of  $H^-$  ions is about five times less intensive than the contribution from the secondary electron processes. This

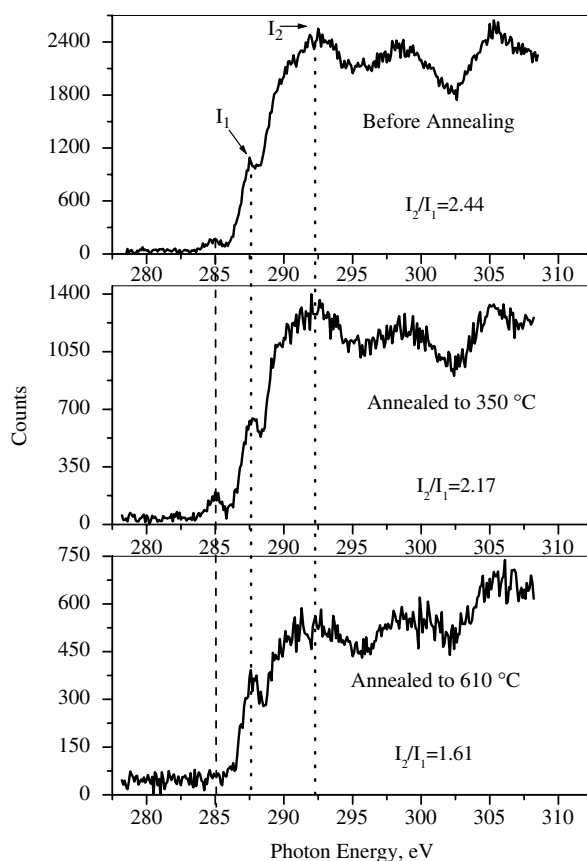


**Figure 9.** Total  $D^+$  PSID yield spectra of the diamond film exposed to MW deuterium plasma as a function of temperature of subsequent annealing (from [27]).

small resonance-driven contribution may be induced by some valence excitations of surface molecular species by electron impact or, alternatively, by the electron attachment from the diamond surface to an H atom or positive ion whose desorption was stimulated by a direct process.

### 5. PSID of surface versus sub-surface deuterium in diamond

$H^+$  PSID was applied to distinguish between surface and sub-surface hydrogen/deuterium in diamond films and study their thermal stability [27]. In figure 9 normalized total  $D^+$  desorption yields from the MW plasma deuterated sample at room temperature and after annealing to 350 and 610 °C are shown as a function of incident photon energy in the 280–310 eV range. Deuteration, instead of hydrogenation, was performed to distinguish between possible adsorption of residual hydrogen gas and intentionally performed deuteration.

The room temperature spectrum consists of a peak at 287.5 eV (with intensity  $I_1$ ) corresponding to the  $C(1s)-\sigma^*$  excitation energy of the carbon atoms bonded to hydrogen, C–H(ads), a broad peak at ~292 eV photon energy (with intensity  $I_2$ ), a dip at 302.4 eV corresponding to the second absolute bandgap of diamond, and a small peak at 285.2 eV, which was earlier attributed to valence band excitations induced by secondary electrons in diamond

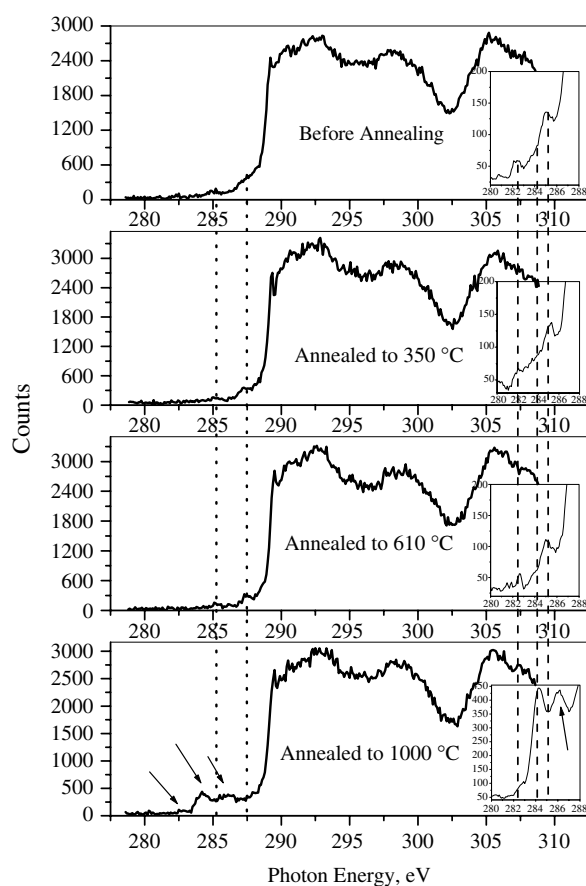


**Figure 10.** 35 eV PEY NEXAFS spectra of the diamond film exposed to MW deuterium plasma as a function of temperature of subsequent annealing. Inset: enlarged view of the spectral region below the carbon absorption edge (from [27]).

layers having some  $sp^2$ -bonding configuration, i.e., layers with open dangling bonds or with atomic dislocations due to defects or partially amorphous structure [28]. It can be observed that annealing to 350 °C results in a substantial decrease in the ratio of  $I_2$  to  $I_1$  peaks, as well as in a decrease of total  $D^+$  desorption yield, as it can be identified by comparing the normalized integral intensities of PSID spectra. Some increase in the intensity of the 285.2 eV peak can be also noticed.

Annealing to 610 °C results in an even more drastic decrease in both the  $I_2/I_1$  ratio and the total yield of  $D^+$ , and in complete disappearance of the 285.2 eV peak. The relative magnitude of the dip at 302.4 eV, however, remains unchanged irrespective of annealing, confirming that no substantial damage to the sample surface occurred [28]. As was expected, after annealing to 1000 °C no  $D^+$  was detected due to complete desorption of deuterium atoms from diamond surface/sub-surface regions.

The respective PEY NEXAFS spectra of the MW-deuterated and subsequently annealed diamond film can be observed in figure 10. The spectral features are generally similar to those present in PSID spectra; however, some exceptions can be noticed. First, a peak at 289.3 eV can be observed in all spectra. This peak is due to the characteristic diamond core exciton, 0.19

eV below the CBM, and it proved to be a fingerprint of diamond crystalline perfection [29]. (In PSID spectra, it is difficult to observe the exciton peak due to the somewhat decreased resolution resulting from optimization of monochromator optics in order to obtain a reasonable  $D^+$  desorption signal, while maintaining low signal-to-noise ratio.) Second, the C (1s)- $\sigma^*$  C-D(ads) resonance at 287.5 eV is displayed as a shoulder, indicating that C-D chemical bonds are present on the very surface, while NEXAFS spectra yield information from several atomic layers. It should be noted that the C-D resonance can be observed after annealing to 350 and 610 °C, but not for the sample annealed to 1000 °C, where all deuterium atoms desorbed. Third, the peak at 285.2 eV can also be observed for the film annealed to 610 °C, although its intensity reduces upon annealing. Annealing to 1000 °C results in the appearance of a well defined peak at 284.2 eV, and two smaller peaks at 286.2 and 282.6 eV. The first two features were previously attributed to  $\pi^*$ -bonding dimers following desorption of hydrogen atoms [30, 31], whereas the low energy peak, positioned below the Fermi level, was claimed to be associated with a surface state due to single dangling bonds existing at sub-monolayer hydrogen coverage of the diamond surface [31].

Careful analysis of the NEXAFS spectrum below the absorption edge, i.e. in the 280–288 eV region (see insets in figure 10), enables detection of the 282.6 eV peak in deuterated samples as well. In addition, for the film annealed to 610 °C, one can see a shoulder at 284.2 eV, which may indicate some desorption of the hydrogen atoms from the surface and formation of  $\pi$ -dangling bonds in the vacant regions. The intensity of this shoulder is very small compared to the corresponding peak after annealing to 1000 °C, confirming that only a small fraction of surface deuterium atoms desorbs at 610 °C.

In figure 11 the normalized  $D^+$  PSID spectra of the *in situ* hot filament (HF) deuterated film following annealing are shown. It was prepared by *in situ* deuteration of the hydrogen-free (bare) surface produced by annealing to 1000 °C. It can be observed that annealing to 350 °C does not induce any detectable changes in the spectral structure, while that of 610 °C results in a small decrease in the integral intensity of the desorption yield spectrum. However, when compared to the PSID spectra of the MW-deuterated film, the total  $D^+$  desorption yield of the film prior to annealing is substantially lower than for the film exposed to the MW plasma, although the ratio  $I_2/I_1$  is higher than for the MW-deuterated one. In addition, the peak at 285.2 eV is not present in the spectra shown in this figure.

From the corresponding NEXAFS spectra shown in figure 12, it can be observed that peaks at 284.2 and 286.2 eV completely disappear following *in situ* HF deuteration, confirming almost full coverage of the surface by deuterium atoms, and the shoulder at 287.5 eV, due to the 1s- $\sigma^*$  C-H(ads) resonance, reappears. In the sub-edge region of the NEXAFS spectra, as displayed in the insets in this figure, the following features can be observed:

- (1) the peak at 285.2 eV with intensity substantially lower than that measured for the sample deuterated by MW plasma and prior to annealing; its height slightly increases upon annealing;
- (2) the peak at 282.6 eV retains similar relative magnitude as for the MW-deuterated samples irrespective of annealing; and
- (3) after annealing of the sample to 610 °C, a very low intensity peak at 284.2 eV can be observed and correlated with the decrease in the total desorption yield of  $D^+$ .

To further correlate between the observed electronic and chemical changes in the diamond film and its electronic properties, a series of secondary electron emission (SEE) spectra was recorded and is shown in figures 13 and 14, representing MW- and HF-deuterated samples, respectively. As can be observed, the onset of electron emission in all cases except for the film annealed to 1000 °C is at 5.4–5.6 eV, which approximately corresponds to the

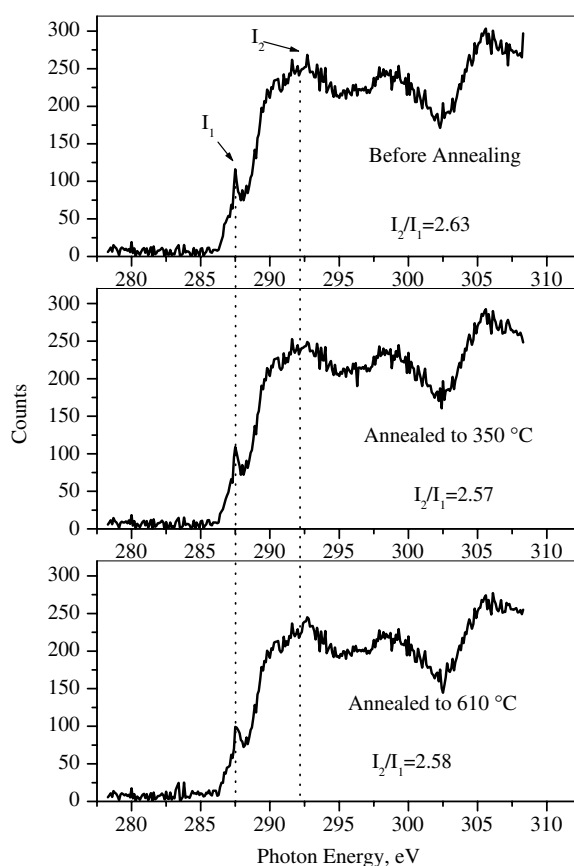


**Figure 11.** Total  $D^+$  PSID yield spectra of the diamond film *in situ* exposed to deuterium gas activated by a hot filament as a function of temperature of subsequent annealing (from [27]).

value of the bandgap in diamond (5.47 eV), and thus indicates NEA, where the electron emission from the conduction band minimum is represented by a sharp peak near the emission threshold [28, 32, 33]. The intensity of this peak, however, substantially decreases following annealing to 610 °C in the case of MW-deuterated film, which also results in an overall decrease in the SEE intensity. This can also be observed for the HF-deuterated surface, however to a lesser extent. The onset of the SEE spectrum of the film annealed to 1000 °C is positively shifted by 0.8 eV, i.e., from 5.5–6.3 eV which is characteristic of a positive EA surface [32], and it displays low electron emission yield. The values of normalized integral intensities of the SEE, as calculated from figures 13 and 14, as well as  $I_2/I_1$ , PSID peak ratio and integral intensity of  $D^+$  desorption yield spectra, as identified from figures 9 and 11, are plotted in figure 15 as a function of annealing temperature for both MW- and HF-deuterated diamond films.

The above results suggest that the effects of *ex situ* MW deuteration and *in situ* HF deuteration differ in the following aspects. Deuterium atoms adsorbed by HF are stable up to 610 °C at least, while the amount of those adsorbed by MW plasma treatment is strongly reduced upon mild heating to 350 °C. A similar behaviour was observed for the  $I_2/I_1$  peak ratio in the PSID spectra. Let us briefly describe the relation between the intensities of these peaks and the dynamics of  $D^+$  ( $H^+$ ) photodesorption. Direct excitation processes result in the appearance of a peak at 287.5 eV, which is the (1s) core-level ionization energy of carbon

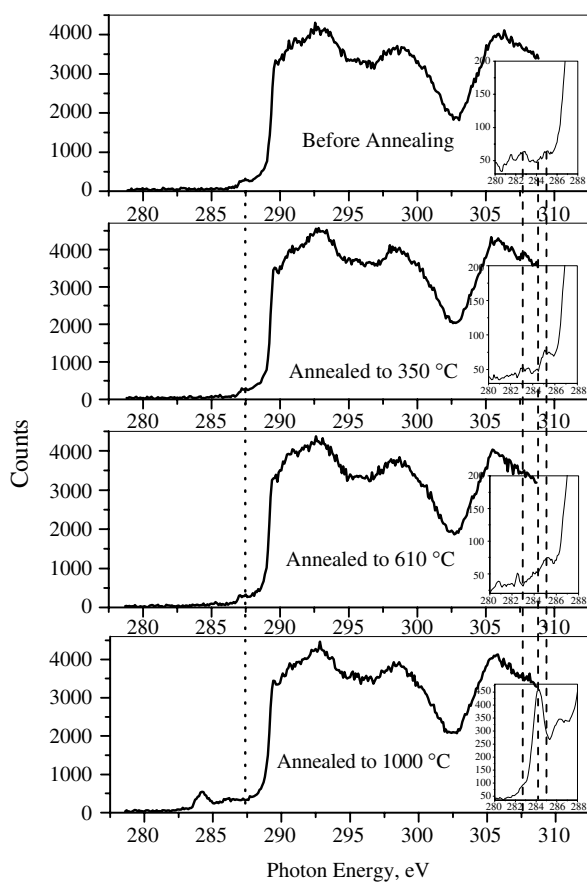


**Figure 12.** 35 eV PEY NEXAFS spectra of the diamond film *in situ* exposed to deuterium gas activated by a hot filament as a function of temperature of subsequent annealing. Insets: enlarged view of the spectral region below the carbon absorption edge (from [27]).

bonded to deuterium (hydrogen) bonds. They induce an additional peak at  $\sim 291$  eV due to C (1s)- $\sigma^*$  resonance transitions in C-C bonds in which carbon atoms are also bonded to hydrogen/deuterium. The relaxation of this core hole may result in the desorption of  $D^+$ . On the other hand, indirect excitation due to secondary electrons produces features similar to the electron PEY NEXAFS spectrum, as shown in figures 10 and 12. We will show in the next chapter that although the peak at 287.5 eV and spectral features at approximately 290–295 eV are contributed by both direct and indirect desorption processes, those located above 290 eV are mostly due to indirect processes, while the peak at  $\sim 285$  eV is entirely due to excitations induced by secondary electrons [28].

It is supposed that C-D chemical bonds in the *in situ* HF-deuterated sample are present on the very surface. Therefore, a decrease in the  $I_2/I_1$  peak ratio for the MW-deuterated film upon annealing indicates a decrease in the number of secondary electron excitations. This decrease is well correlated with the decrease in the intensity of SEE as observed from figure 13. For the HF-deuterated film, this ratio is nearly constant, and a decrease of SEE intensity upon annealing is lower than for the MW-deuterated film. As discussed below, this difference is associated with the presence of some sub-surface deuterium in the case of MW plasma treatment and its relatively low thermal stability at moderate heating.

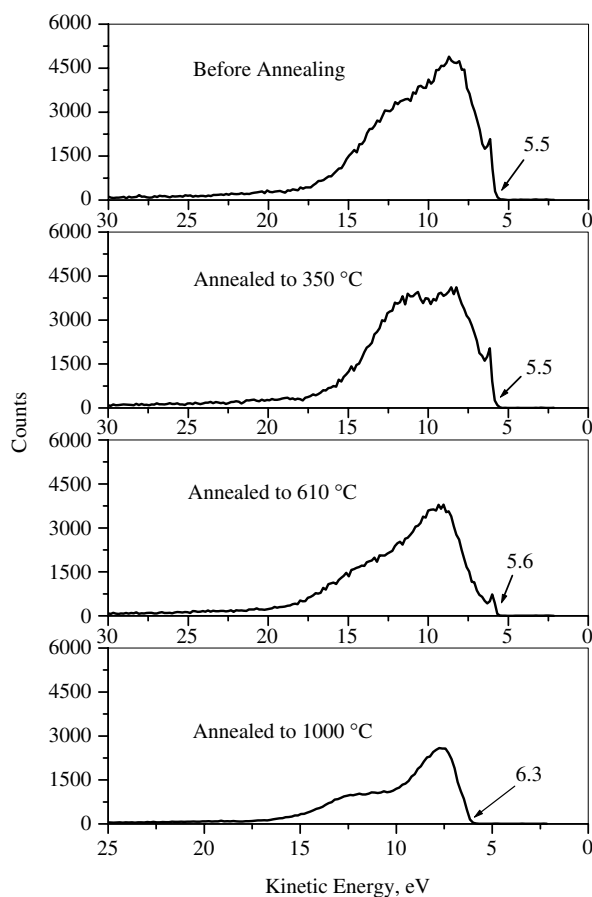


**Figure 13.** SEE spectra of the diamond film exposed to MW deuterium plasma as a function of temperature of subsequent annealing. The energy scale is determined with respect to the Fermi level of the sample. The onset of the emission is marked by an arrow (from [27]).

A decrease in total  $D^+$  PSID yield upon annealing can be explained by a reduction in the total amount of deuterium in the diamond film. It is well known, however, that C–D chemisorbed bonds are stable up to  $\sim 800^\circ\text{C}$  [20, 34]. Therefore, such a strong decrease in the  $D^+$  desorption yield in the MW-deuterated sample is most probably caused by desorption of weakly bonded sub-surface or bulk deuterium. It can be supposed that desorption of these atoms at moderate heating ( $350^\circ\text{C}$ ) can induce some atomic dislocations in the near-surface region, leading to an increase in the relative intensity of the peak at 285.2 eV in the PSID spectrum. Annealing to a higher temperature ( $610^\circ\text{C}$ ) removes defects in diamond structure to some extent: this is why the intensity of this peak decreases. In the case of HF-deuterated samples, the total number of deuterium atoms remains nearly constant upon annealing to  $350^\circ\text{C}$ , and somewhat reduces when the film is heated to  $610^\circ\text{C}$ . On the basis of these data and the fact that the  $I_2/I_1$  ratio does not change, it can be concluded that in situ HF deuteration results in the adsorption of deuterium on the very surface without substantial penetration to sub-surface layers. This is consistent with the lower desorption yield of  $D^+$  of HF- as compared to MW-deuterated film. Defects on the surface of polycrystalline films originated from grain boundaries can result in production of some relatively weakly bonded deuterium which desorbs



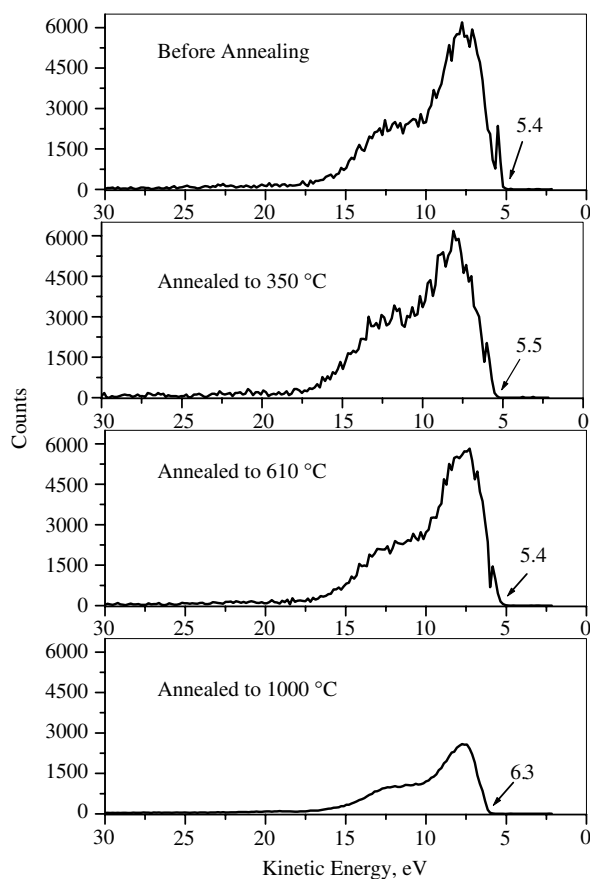


**Figure 14.** SEE spectra of the diamond film *in situ* exposed to deuterium gas activated by a hot filament as a function of temperature of subsequent annealing. The energy scale is determined with respect to the Fermi level of the sample. The onset of the emission is marked by an arrow (from [27]).

at temperatures lower than 800 °C [34]. This can explain the slight reduction in the  $D^+$  desorption yield in the HF-deuterated film after heating to 610 °C. This process is reflected by the appearance of the shoulder at 284.2 eV in NEXAFS spectra, which corresponds to the formation of  $\pi$ -bonded dangling bonds following hydrogen (deuterium) desorption, and results in a decrease of SEE intensity. The last effect is evident, as surface hydrogen is well known to enhance the electron emission properties of diamond. We would like to point out that partial desorption of deuterium did not result in a detectable increase in the intensity of the small peak at 282.6 eV in NEXAFS spectra, as shown in the insets in figures 10 and 12. As was noted above, this peak can be observed for all fully and partially hydrogenated and hydrogen-free diamond surfaces. Hence, although excitonic in origin because of its location below the Fermi level, it cannot be unambiguously referred to the formation of single dangling bonds on the partially hydrogenated diamond surface [31].

## 6. PSID from hydrogenated ion-beam damaged diamond surfaces

$H^+$  PSID was applied to investigate diamond surfaces exposed to low energy ion beams [28]. The ion irradiation was performed at room temperature using 30 keV  $Xe^+$  ions at three doses:

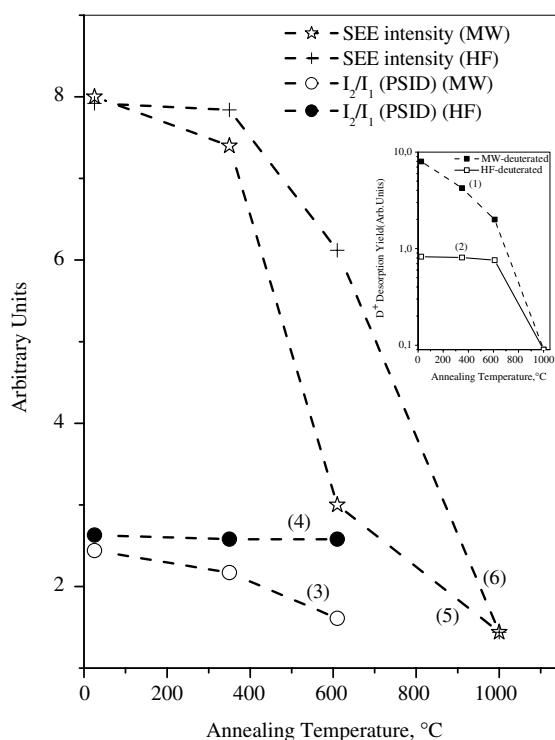


**Figure 15.** Normalized integral  $D^+$  PSID yield (curves 1 and 2 in the inset),  $I_2/I_1$  PSID peak ratio (lines 3 and 4), and normalized integral SEE intensities (lines 5 and 6) of MW and hot filament deuterated diamond films, respectively, as a function of annealing temperature (from [27]).

$2 \times 10^{13}$  ('low dose'),  $2 \times 10^{14}$  ('medium dose'), and  $2 \times 10^{15}$  ions  $\text{cm}^{-2}$  ('high dose'). The distribution of the defects in the near-surface region, as calculated using the TRIM computer program, extends from the surface to a depth of  $\sim 100$  Å. These doses result in the formation of point defects in the crystalline diamond matrix, a large degree of disordered  $\text{sp}^3$ -bonded structure, and a fully amorphous, mainly  $\text{sp}^2$ -bonded carbon material, respectively [35]. As in the previous case,  $\text{H}^+$  PSID spectra are correlated with the PEY NEXAFS measurements.

In figures 16(a) and (b) NEXAFS spectra measured using 8 and 35 eV secondary electrons, respectively, for the four different films studied (three ion-bombarded and the unimplanted one) are shown. The spectral features measured for the unimplanted diamond film are attributed to high-quality diamond. In particular, a sharp peak at 289.2, 0.2 eV below the carbon absorption edge corresponds to a characteristic diamond core exciton; a dip at 302.4 eV is attributed to the second absolute bandgap; structures around 293 eV are associated with the  $\text{C}(1s)-\sigma^*$  (C-C) transitions. The NEXAFS spectrum of the unimplanted film measured using 35 eV electrons shows an additional low intensity peak at 287.5 eV, a  $\text{C}(1s)-\sigma^*$  resonance in C-H. No  $\text{sp}^2$ -related peaks, which generally appear in the pre-edge region, are observed, indicating the very good quality of the as-deposited film. NEXAFS spectra obtained from the low dose implanted sample seem to be similar to those of the unimplanted diamond. However, careful examination enables one to distinguish several deviations between the spectra. First, the intensity of the diamond core exciton peak is significantly lower, and it was obtained, in this case, only when the best resolution conditions were applied to the incident photon beam. Second, two additional peaks appear in the pre-edge energy region: a small one at 285.5 eV assigned to the  $\text{C}(1s)-\pi^*$

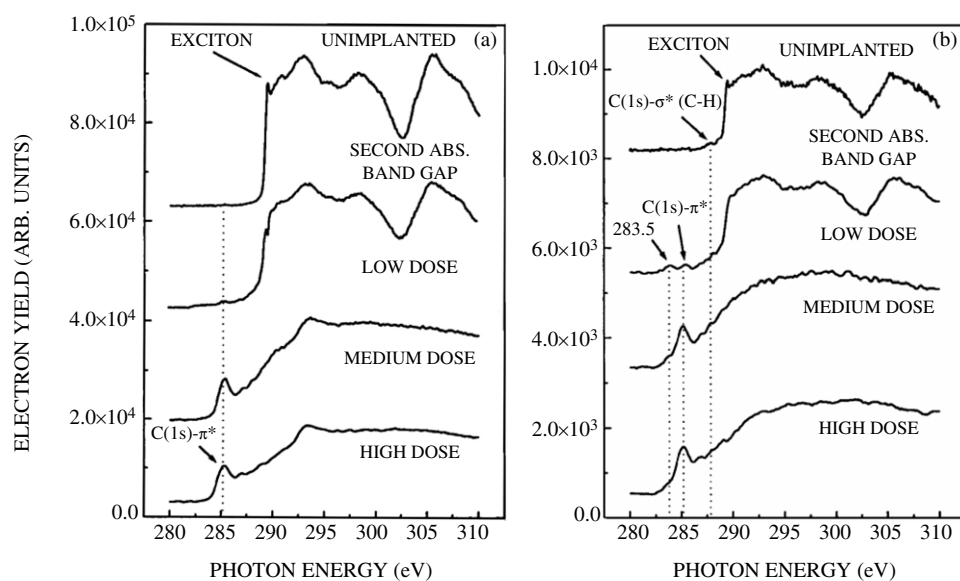


**Figure 16.** PEY NEXAFS spectra of implanted and unimplanted diamond films measured using (a) 8 eV and (b) 35 eV secondary electrons (from [28]).

transition, corresponding to  $sp^2$  graphite-like carbon, and a peak centred at 283.5 eV. This last peak was attributed to the formation of defective acceptor states 0.2 eV above the valence band maximum [29]. The pre-edge structures are less prominent in the NEXAFS spectrum obtained using 8 eV secondary electrons compared to that obtained using 35 eV secondary electrons, suggesting that the defective layer is localized in the near-surface region.

The NEXAFS spectra measured for the samples implanted to medium and high doses (in both the surface- and bulk-sensitive modes) almost completely lose the spectral features characteristic of diamond. These spectra show a growing C(1s)- $\pi^*$  peak at 285.5 eV with a shoulder on the low-energy side. This shoulder most likely is associated with the 283.5 eV peak clearly resolved for the low-dose implanted sample. It should be noted that the peak at 287.5 eV, attributed to a C-H(ads) resonance, could still be observed as a shoulder in the 35 eV NEXAFS spectra from implanted samples.

For further elucidation of the effect of ion bombardment on the PSID of  $H^+$ , SEE measurements of the implanted films were conducted, of which the results are shown in figure 17. The SEE spectra of the unimplanted diamond film show a sharp and relatively intense peak at 5.5 eV. Considering that the kinetic energies were measured with respect to the Fermi level and this is positioned very close to the valence band maximum [36], emission of electrons with energy of 5.5 eV, which is about the value of the absolute bandgap of diamond, corresponds to the emission of electrons thermalized to the conduction band minimum. Such emission may occur only in the case when the vacuum level is located below the conduction band minimum, indicating NEA [17, 37]. The SEE spectra of implanted films are characterized by

- (i) a positive shift of the emission threshold to 6.6–6.7 eV, thus placing the position of the vacuum level more than 1 eV above the conduction band minimum;
- (ii) a decrease of the emission intensity by a factor of 2.5 for the sample implanted at low ion dose, and by a factor of 5 for the diamond samples irradiated at higher ion flux.

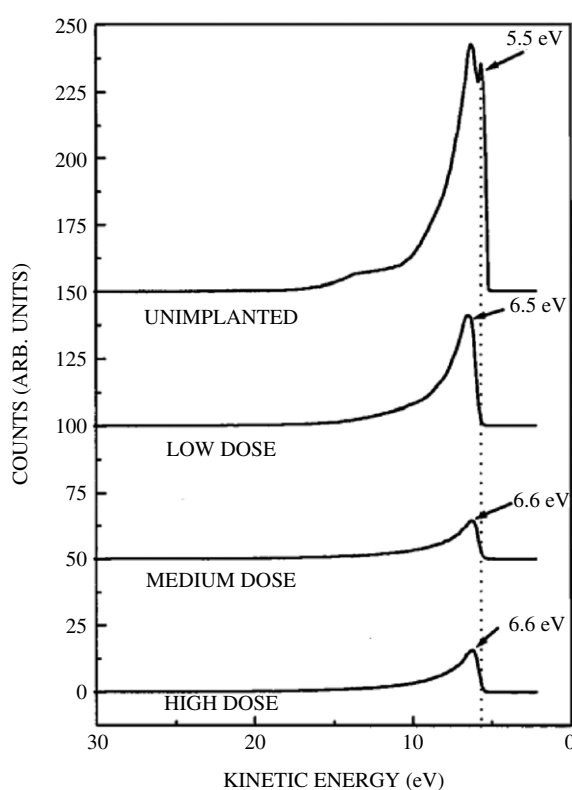
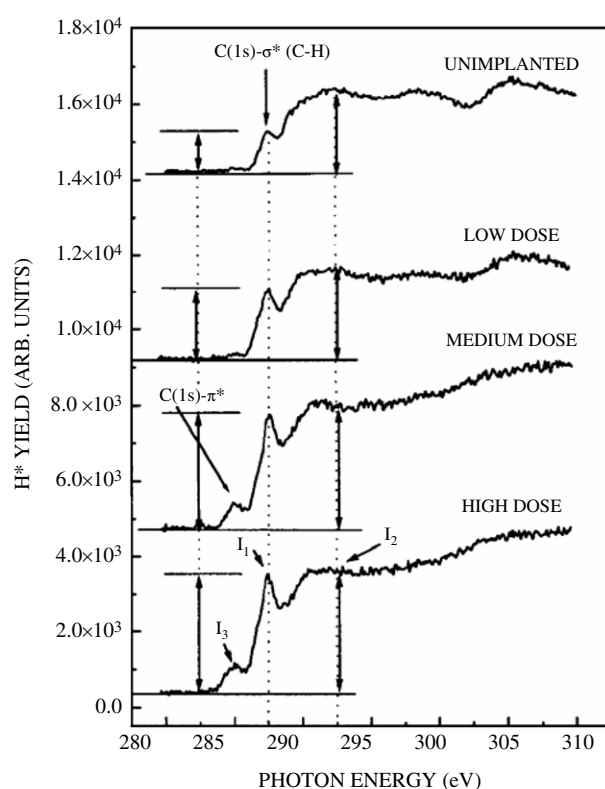


Figure 17. SEE spectra of implanted and unimplanted diamond films (from [28]).

The positive shift of the emission threshold indicates the conversion of the EA from negative to positive. The decrease in intensity of the SEE yield induced by ion irradiation of diamond surfaces is characteristic of damaged and disordered diamond [38, 39]. These results suggest that surface processes driven by low energy secondary processes are expected to be reduced for the implanted as compared to the unimplanted films.

In figure 18 the desorption yields of  $H^+$  as a function of photon energy in the 280–310 eV range for the different samples are shown. A peak corresponding to the  $C(1s)-\sigma^*$  excitation energy of the carbon atoms bonded to hydrogen,  $C-H(ads)$ , at 287.5 eV (with intensity  $I_1$ ) is present in all spectra, and its relative intensity for the implanted samples is higher than for the unimplanted diamond film with  $I_1 = 1300$ , compared to that of the low, medium, and high dose implanted films, displaying values of 1600, 2000, and 2250, respectively. For the implanted samples a broad peak is observed at about 291 eV photon energy. At higher photon energies the PSID yield is similar to that of the electron NEXAFS, with a maximal intensity indicated as  $I_2$  (measured at 292.5 eV). In this energy range the PSID yield is very different for the implanted films compared to the unimplanted sample. The dip corresponding to the second absolute bandgap of diamond at 302.4 eV is already largely washed out by a background signal for the sample implanted at a low  $Xe^+$  dose, indicating that a considerable part of the diamond surface is damaged. Also, the intensity  $I_2$  relative to  $I_1$  gradually decreases as the implantation dose increases: for the unimplanted film  $I_2/I_1$  is 1.98, whereas for the films implanted at low, medium, and high ion doses  $I_2/I_1$  is 1.25, 1.11, and 1.0, respectively. In addition, one can observe a peak at 285.5 eV, marked as  $I_3$ , whose intensity increases with



**Figure 18.** Total photo-desorption yield of H<sup>+</sup> ions as a function of incident photon energy for implanted and unimplanted hydrogenated diamond films (from [28]).

the implantation dose. In figure 19 the intensities  $I_1$ ,  $I_2$ , and  $I_3$  of the three peaks are plotted as functions of the ion dose. The appearance of the 285.5 eV peak in the PSID spectra of implanted samples, marked as  $I_3$ , is most likely due to hydrogen ion desorption promoted by valence band excitations induced by secondary electrons produced solely within the damaged layer and not due to a direct excitation process. This is likely considering that the 285.5 eV peak originates from resonance adsorption processes by double-bonded carbon atoms within the damaged layer. Therefore, its intensity in the PSID spectra of the implanted samples is considered to be almost directly proportional to the contribution of secondary processes to the PSID process. Below, this assumption is quantitatively justified.

The contribution of direct processes may be estimated by subtracting the contribution of indirect processes (i.e., those driven by secondary electrons) from the PSID curves shown in figure 18. This is performed by subtracting the normalized PEY NEXAFS spectra measured using 35 eV secondary electrons (surface sensitive mode) from the PSID spectra of the respective implanted samples. The NEXAFS spectrum measured using 35 eV electrons is used in this calculation, as it is estimated that secondary electrons of energies above ~20 eV have enough energy to induce C-H(ads) valence-band excitation that may lead to hydrogen ion desorption (see [18] and references therein). The normalization is carried out by setting the intensity of the 285.5 eV peak equal in the NEXAFS and PSID spectra of respective samples. This procedure is justified assuming that the 285.5 eV peak in the PSID spectra is solely due to the contribution of secondary electrons to the photo-desorption process. For the unimplanted

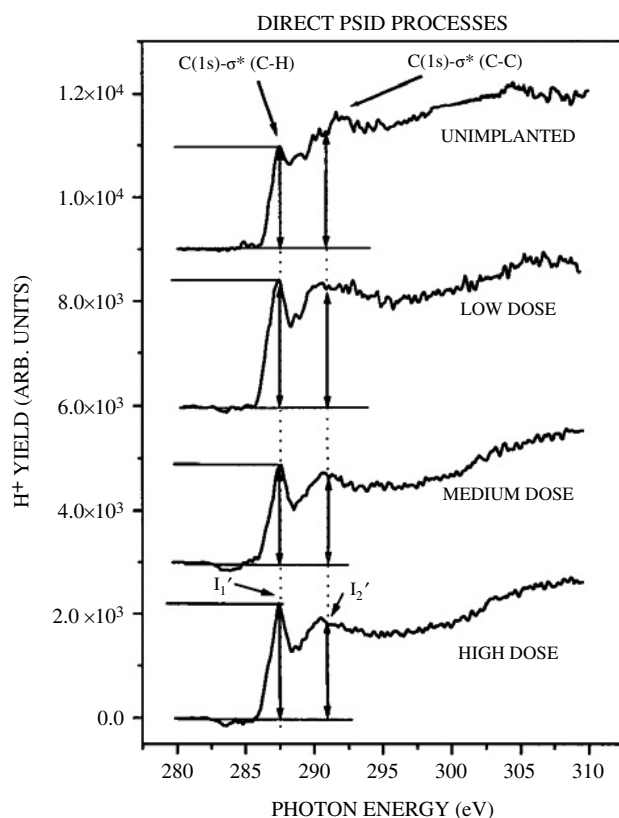


**Figure 19.** Contribution of direct excitation processes to the hydrogen PSID. The curves were obtained by subtracting the normalized 35 eV PEY NEXAFS spectra from the corresponding PSID curves. For the implanted samples, normalization was carried out with respect to the 285.5 eV peak. For the unimplanted sample normalization was performed with respect to the dip at 302.4 eV (from [28]).

sample the normalization was carried out by setting the intensity of the 302.4 eV peak equal in both spectra as described in [18]. The results of these operations are shown in figure 19.

As observed from figure 19 the direct PSID process is characterized by a peak at 287.5 eV, marked as  $I_1'$ , and a broader peak at  $\sim 291$  eV, marked as  $I_2'$ , followed by a monotonically increasing dependence of the PSID on photon energy. In figure 20 the  $I_1'$  and  $I_2'$  intensities are plotted as functions of the implantation dose. As observed from this figure, after subtraction of secondary processes, the absolute intensity of the 287.5 eV peak obtained for all implanted samples,  $I_1'$ , is of similar intensity (within 10%). Considering that  $I_1'$  originates from direct excitation processes, it is reasonable to assume that its intensity is, to a good approximation, proportional to the H(ads) coverage. This result shows that ion implantation within the above ion doses and energy does not result in a significant loss of adsorbed hydrogen.

Next the authors consider the nature of the broad peak centred at  $\sim 291$  eV, clearly seen in the spectra associated with the direct desorption process marked as  $I_2'$ . A broad peak was measured in the NEXAFS spectra of unconjugated hydrocarbon compounds like  $C_2H_6$  and associated with the C (1s)- $\sigma^*$  (C-C) resonance transition [40]. Therefore, the 291 eV peak in the direct H<sup>+</sup> PSID spectra is due to C (1s)- $\sigma^*$  (C-C) resonance transitions of carbon atoms one of whose bonds is hydrogenated. The relaxation of this C (1s) core hole results in H<sup>+</sup>

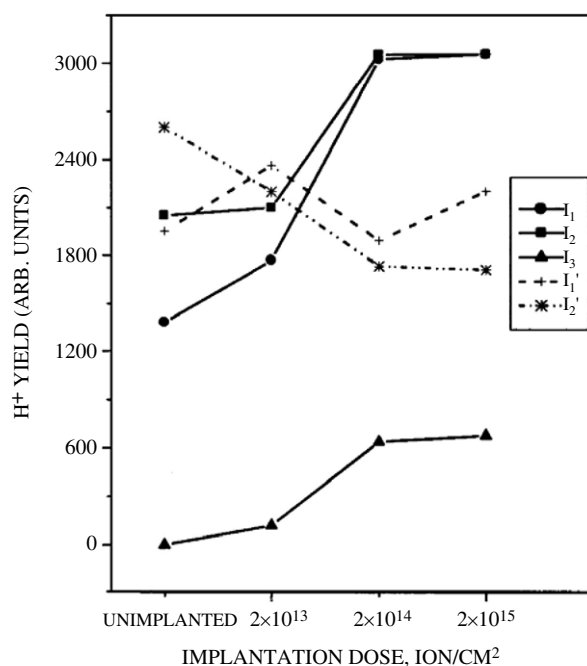


**Figure 20.** Intensities of the  $I_1$ ,  $I_2$ , and  $I_3$  peaks as measured in the PSID spectra shown in figure 18, and intensities of the  $I'_1$  and  $I'_2$  peaks as measured from the direct contribution to the PSID processes, shown in figure 19 (from [28]).

desorption [18]. As seen from figure 19, the intensity of the PSID yield at energies higher than  $\sim 290$  eV is lower for the implanted samples as compared to the unimplanted one, and decreases with the implantation dose. Considering that in this energy range secondary electron processes contribute to the PSID yield, it may be concluded that the contribution of these processes to the emission of positive hydrogen ions decreases with increasing damage of the diamond surface. This is reflected by the decrease in the  $I_2/I_1$  ratio with the implantation dose. In particular, the intensity ratio between features in the PSID solely associated with indirect processes and those associated with direct processes is expected to scale with the relative reduction in secondary electron yield with a  $\sim 1:1$  correspondence. This is so because for the hydrogenated diamond film (unimplanted film) the efficiency of direct and indirect processes was determined to be  $\sim 1:1.7$ . From these experimental results and analysis the ratio between the 285.5 eV peak  $I_3$  for the medium and high dose implanted samples and the corresponding 287.5 eV peak as measured from the direct PSID spectra,  $I'_1$ , is similar to the ratio of SEE yield between the unimplanted and implanted samples. This agreement strongly supports the assumption that the 285.5 eV peak in the PSID spectra is due to indirect processes.

### 7. Interaction of thermally activated and molecular oxygen with hydrogenated polycrystalline diamond surfaces

$H^+$  PSID measurements were used to clarify chemical bonding modifications due to interactions of the hydrogenated diamond surface with thermally activated and molecular oxygen [41]. In figure 21 XPS graphs of the hydrogen-terminated diamond surface before and after exposure to oxygen are shown. From the spectra shown in figure 21(a) it can be seen that

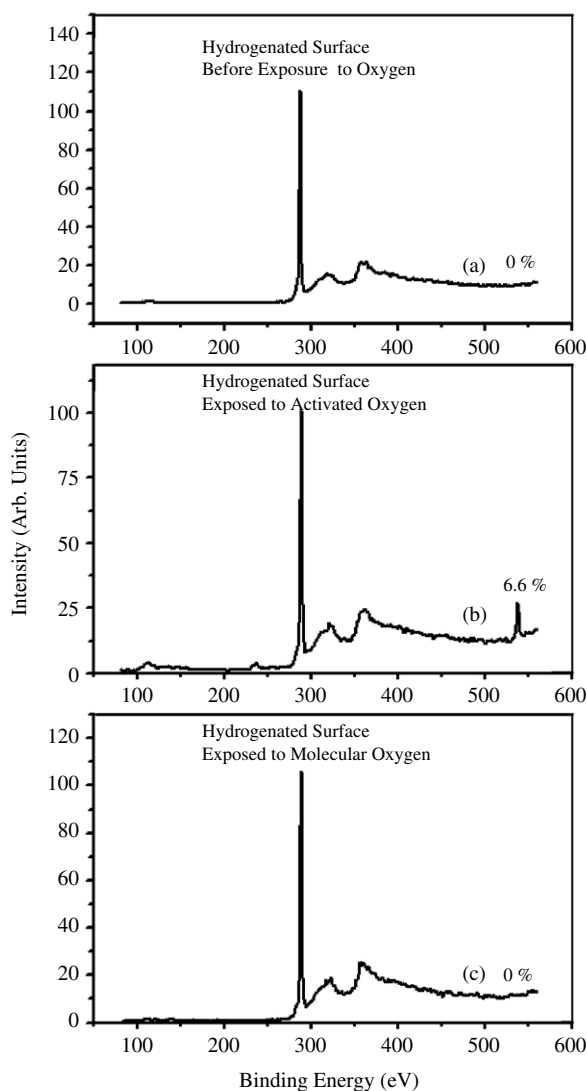


**Figure 21.** XPS spectra of the hydrogen terminated diamond film before (curve a) and after exposure to thermally activated (curve b) and molecular (curve c) oxygen (from [41]).

the as-hydrogenated diamond surface is free of impurities (down to the detection limit of XPS) and the satellites associated with the C (1s) can be associated to the characteristic diamond bulk and surface plasmons. An identical spectrum was obtained for the hydrogenated surface after exposure to molecular oxygen. For a sample exposed to activated oxygen, XPS shows a clear O (1s) peak at 532 eV, and the estimated concentration of oxygen atoms relative to carbon is 6.6% (hydrogen atoms cannot be taken into account since they are not detected by XPS). This value is obtained by using relative x-ray ionization cross sections for carbon and oxygen at 630 eV excitation energy [42], and assuming homogeneous distribution of oxygen atoms through the detection depth of XPS (20–50 Å). The actual atomic concentration of oxygen may be substantially higher if adsorbed only on the uppermost atomic layer.



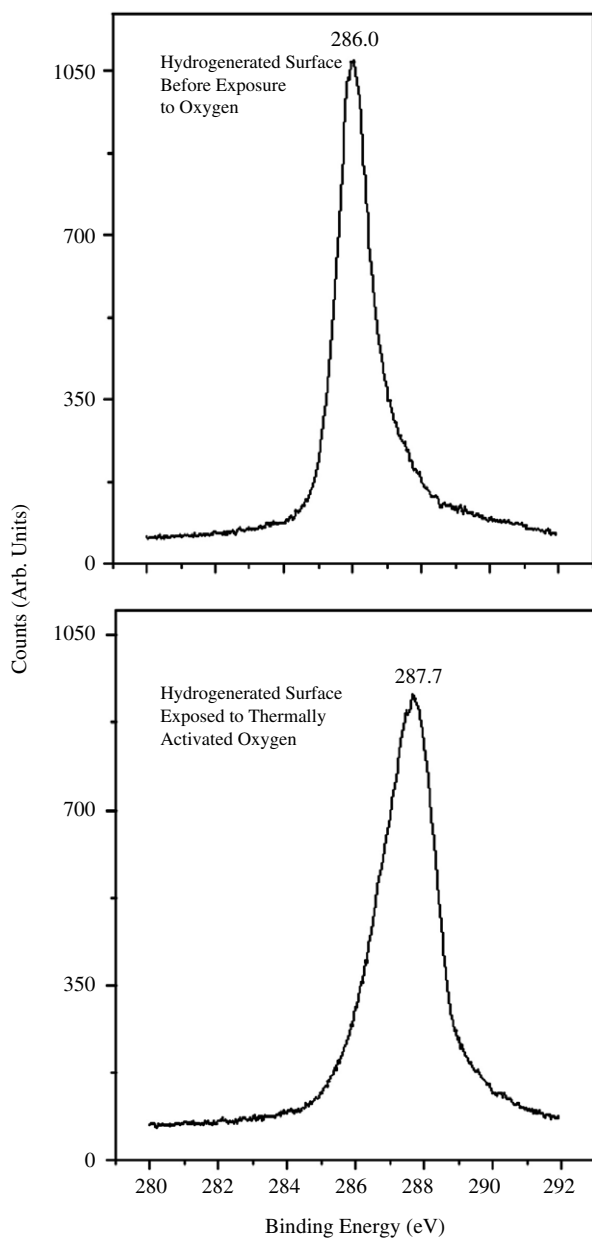


**Figure 22.** High resolution XPS spectra of the hydrogen terminated diamond film around the C (1s) binding energy peak measured (a) before and (b) after exposure to thermally activated oxygen (from [41]).

In figure 22 high resolution XPS spectra around the C (1s) peak are shown. The C (1s) binding energy of the thermally oxidized sample is positively shifted by 1.7 eV as compared to that of the as-hydrogenated one, while molecular oxygen has no effect on its position (data not shown). One would also note the broadening of the C (1s) peak from 1.3 eV (FWHM) to 1.9 eV after thermal oxidation. In figure 23 PEY NEXAFS spectra of the diamond

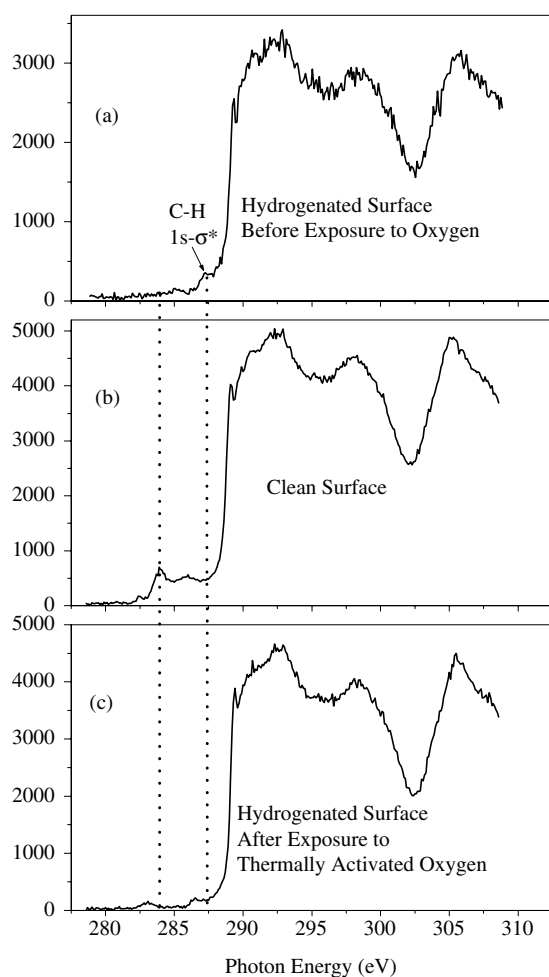


**Figure 23.** PEY NEXAFS spectra of diamond film surfaces: (a) hydrogenated surface; (b) clean surface; (c) hydrogenated surface after exposure to thermally activated oxygen (from [41]).

films around the carbon K-edge are shown. As expected, all these spectra display a sharp peak at 289.3 eV characteristic of the core exciton of diamond and a dip at 302.4 eV that corresponds to the second absolute bandgap in the diamond electronic structure [30]. As has been shown previously, both spectral features are fingerprints of the pristine character of diamond crystallites and are drastically affected by defects [28]. In the case of the hydrogenated diamond film, the shoulder at 287.5 eV is associated with the C (1s)- $\sigma^*$  resonance in C-H bonds. This shoulder disappears after exposure of the film to thermally activated oxygen.

The analysis of the pre-edge features in NEXAFS spectra can be used to determine the presence of defects, dangling bonds or  $sp^2$ -bonded, graphite or amorphous carbon in the near-surface region. The reference spectrum of the diamond film annealed to 1000 °C (all surface adsorbates are removed upon such a treatment, producing a clean diamond surface) displays two peaks in this region that are not present in the corresponding spectrum of the hydrogenated film: a relatively strong peak at 284.2 eV and a weaker one at 286.2 eV. These peaks were attributed to  $\pi$ -bonded dimers following the full or even partial desorption of

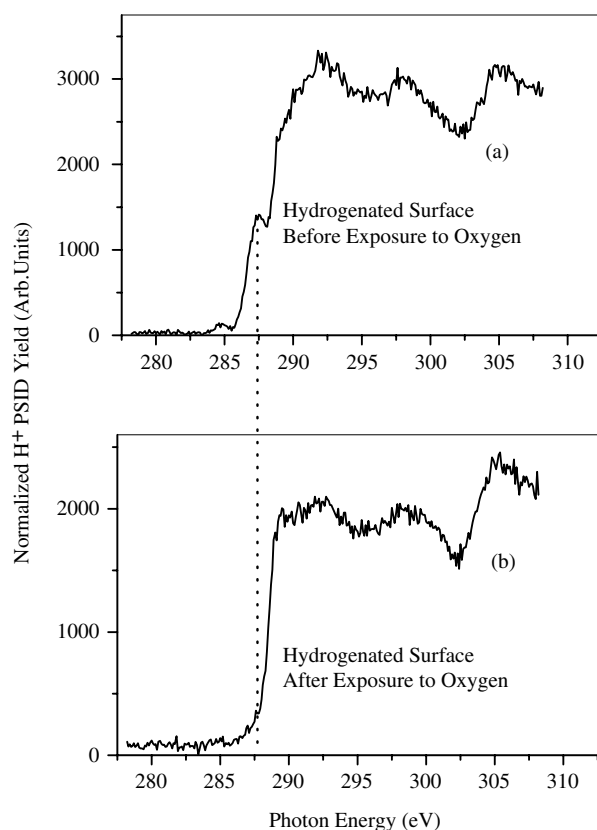


**Figure 24.** Carbon K edge  $H^+$  PSID spectra of the hydrogen terminated diamond surface: (a) before and (b) after exposure to thermally activated oxygen (from [41]).

hydrogen atoms [31]. Exposure of the hydrogenated diamond surface to molecular oxygen did not induce any changes in this part of the spectrum, while thermally activated oxygen produced a very small peak at 286.6 eV which is characteristic of the  $C(1s)-\pi^*$  resonance in  $C=O$  [43].

$H^+$  carbon K edge PSID spectra for the hydrogenated diamond surface before and after exposure to oxygen are shown in figure 24. The spectrum taken immediately after hydrogenation, as well as after filling the chamber with oxygen gas without activation, displays a well defined peak at 287.5 eV due to the direct desorption process through a  $C(1s)$  core-hole excitation of carbon atoms bonded to hydrogen ( $C-H$ ) [18, 20]. This peak disappears after treatment of the surface with activated oxygen gas, and the  $H^+$  PSID curve shows only spectral features due to indirect  $H^+$  desorption processes initiated by valence band excitations induced by secondary electrons which are produced in diamond as a result of photoelectron excitation: these structures are, however, less pronounced than in the case of the as-hydrogenated film. In addition, the integral intensity of the  $H^+$  desorption yield decreases by  $\sim 20\%$  following such an exposure. The decrease in the  $H^+$  PSID yield is difficult to correlate to the amount of adsorbed hydrogen because the PSID process involves secondary electrons and their yield is affected by adsorption of oxygen.

In figure 25 the  $H^+$  PSID spectrum near the oxygen K edge is shown for the film exposed to activated oxygen gas. This spectrum consists of a single peak at  $\sim 541$  eV, which corresponds to the core-level ionization energy of oxygen atoms bonded to hydrogen [43]. It should be noted

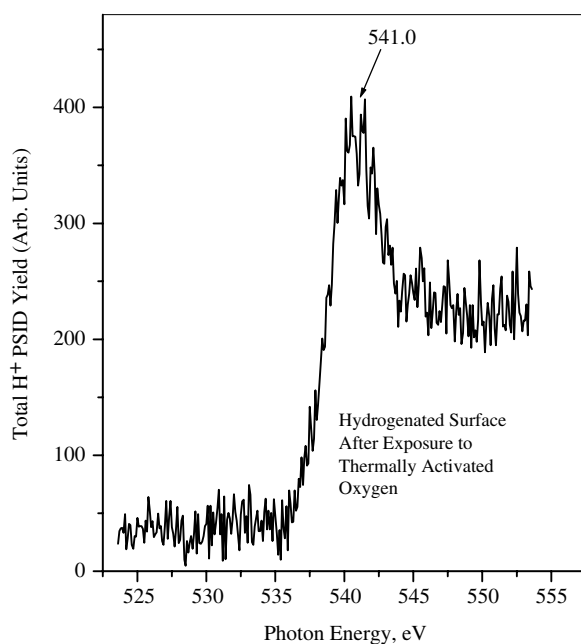


**Figure 25.** The oxygen K edge  $H^+$  PSID spectrum of the hydrogen terminated diamond surface after exposure to thermally activated oxygen (from [41]).

that no signal was obtained in this energy range when measuring  $H^+$  PSID after exposure of the hydrogenated surface to molecular oxygen.

These results clearly indicate that molecular oxygen does not adsorb (either chemically or physically) on the hydrogen-terminated diamond surface at the conditions applied in our work. On the other hand, this surface is reactive to thermally activated oxygen molecules. In this case oxygen atoms are chemisorbed, as revealed from the PSID measurements, showing structures characteristic of chemically bonded surface oxygen, and XPS spectra which display a shift and broadening of the C (1s) peak to a higher binding energy. These changes in the C (1s) line shape and energy position are most likely associated with two effects: (i) modification of the oxidation state of carbon and (ii) changes in surface band bending induced by oxygen adsorption [31, 44].

Possible processes and chemical changes in the state of the hydrogenated diamond surfaces are discussed. (i) Activated oxygen gas can induce full or partial denuding of the surface. This process, however, does not take place, as verified by the NEXAFS spectrum shown in figure 23 (curve c), which would display a well defined peak at 284.2 eV should the adsorbate-free surface have been produced. (ii) Oxygen atoms can induce abstraction of chemisorbed hydrogen atoms and production of various bonding configurations involving carbon and oxygen (most probably carbonyl bonds). The existence of such a process was proved by high resolution electron energy loss spectroscopy measurements [45–48]. This reaction seems to occur in our case as well, as can be deduced from the presence of the 286.6 eV peak in the corresponding NEXAFS spectrum (see curve c in figure 22) due to the C (1s)– $\pi^*$  resonance in C=O (ads), but it is not a dominant process, as it can be concluded on the basis of NEXAFS spectra of oxidized diamond surfaces near the oxygen K edge [49]. (iii) Formation of C–O–H surface bonds. The predominant formation of such C–O–H bonds is supported on the basis of PSID results and discussed below.

The integral  $H^+$  desorption yield is proportional to the concentration of hydrogen on the substrate surface. It can be observed that the normalized integral intensity of the PSID spectrum taken after exposure of the film to thermally activated oxygen decreases only by  $\sim 20\%$  as compared to the as-hydrogenated surface. Considering that the  $H^+$  PSID processes are partially due to valence band excitations driven by secondary electrons and that the SEE yield decreases by  $\sim 20\%$  following oxidation [49], it is concluded that the absolute amount of adsorbed hydrogen does not substantially decrease following the interaction of activated oxygen with the hydrogenated surfaces. The question that can be asked at this point is what the bonding configuration is of hydrogen following adsorption of activated oxygen. First, hydrogen can fully or partially retain its previous bonding, i.e. direct bonding to carbon: in this case all or most of the chemisorbed oxygen atoms are also directly bonded to surface carbon on the hydrogen-free part of the surface. The second possibility is production of the surface C–O–H bonds. The formation of C–O–H upon exposure to activated oxygen is unambiguously proved by the PSID spectrum in figure 25: the 541 eV peak in the  $H^+$  ion yield is due to the core level excitation of O–H bonds [43]. Now, when analysing the PSID spectrum near the carbon K edge (figure 24), we can conclude that only the latter hydrogen bonding configuration exists. This is due to the total disappearance of the 287.5 eV peak corresponding to C–H(ads). On the basis of the dynamics of  $H^+$  PSID from diamond discussed in the previous section, it was concluded that the 287.5 eV peak is contributed mainly by C (1s) excitation processes of carbon atoms bonded to chemisorbed hydrogen resulting in breaking of C–H(ads) bonds. Hence, the ultimate condition for its appearance is the presence of C–H bonds. In the case of their absence, the only possible channel for  $H^+$  desorption by 280–310 eV photon irradiation is through excitations of valence band electrons in the near-surface region of diamond (the indirect desorption process). It was proved that such excitations produce a desorption yield spectrum similar to the NEXAFS spectrum of diamond measured in the reflective PEY mode, i.e. showing a dip at 302.4 eV, which is due to the second absolute bandgap in the diamond electronic structure, and peaks in the 290–295 eV region produced by  $(1s)-\sigma^*$  transitions in C–C. Then the desorbing  $H^+$  ions originate from H not directly bonded to carbon atoms, thus supporting the formation of the C–O–H bonding configuration.

## 8. Conclusions

Hydrogen PSID is a powerful tool for study of local electronic bonding, chemical structure and thermal stability of surface and sub-surface hydrogen on diamond as well as its interactions with other species. Its utilization, however, requires detailed understanding of the mechanism and dynamics of the desorption processes.

We demonstrated in this review paper that the bonding configuration of adsorbed hydrogen or deuterium atoms can be elucidated. PSID measurements performed after annealing to different temperatures were used to distinguish between surface and sub-surface hydrogen which showed a principal difference between *ex situ* hydrogenation by MW hydrogen plasma, and the *in situ* process by passing hydrogen gas through a hot tungsten filament at high vacuum conditions. It is also shown that the amount of adsorbed hydrogen on the diamond surface is a key factor in its electron emission properties and activation of the NEA.

Using  $H^+$  PSID spectroscopy we were able to study damage induced by a low dose  $Xe^+$  ion bombardment and relate it to a strong decrease in electron emission properties of ion-bombarded diamond films.

On the basis of core level PSID and XPS measurements it was concluded that the hydrogen-terminated diamond surface is stable to molecular (unactivated) oxygen but reactive to the thermally activated oxygen gas. Thermally activated oxygen at the conditions applied in

this work chemisorbs resulting in some abstraction of hydrogen with production of C=O (ads), but mainly induces the formation of C–O–H(ads) bonds on the diamond surface. This process is also associated with some decrease in the SEE intensity and production of the PEA surface.

## Acknowledgments

We are thankful to G Dujardin, L Hellner and G Comtet for useful discussions, scientific collaboration and for providing their experimental set-up and assistance in synchrotron radiation measurements. This work was partially supported by the Israel Science Foundation.

## References

- [1] Menzel D and Gomer R 1964 *J. Chem. Phys.* **41** 3311
- Redhead P A 1964 *Can. J. Phys.* **42** 886
- [2] Sanche L 1984 *Phys. Rev. Lett.* **53** 1638
- [3] Ramsier R D and Yates J T Jr 1991 *Surf. Sci. Rep.* **12** 243
- [4] Avouris P and Walkup R E 1989 *Ann. Rev. Phys. Chem.* **40** 198
- [5] Baragiola R A and Madey T E 1991 *Interaction of Charged Particles with Solids and Surfaces (NATO Advanced Study Institute, Series B: Physics vol 271)* ed A Gras-Marti *et al* (New York: Plenum) p 313
- [6] Lanzilloto A M, Madey T E and Baragiola R A 1991 *Phys. Rev. Lett.* **67** 232
- [7] Petravac M 1993 *Phys. Rev. B* **48** 2627
- [8] Petravac M and Williams J S 1995 *J. Vac. Sci. Technol. A* **13** 26
- [9] Hoffman A, Moss S D, Paterson P J K and Petravac M 1995 *J. Appl. Phys.* **78** 6858
- [10] Petravac M, Williams J S and Hoffman A 1996 *Phys. Rev. B* **53** R4257
- [11] Hoffman A and Petravac M 1996 *Phys. Rev. B* **53** 6996
- [12] Morin P and Nenner I 1986 *Phys. Rev. Lett.* **56** 1913
- [13] Lapiano-Smith D A, Ma C I, Wu K T and Hanson D M 1989 *J. Chem. Phys.* **90** 2162
- [14] Lablanquie P, Souza A C A, de Souza G G B, Morin P and Nenner I 1989 *J. Chem. Phys.* **90** 7078
- [15] Rosenberg R A 1986 *J. Vac. Sci. Technol. A* **4** 1463
- [16] Ramaker D E 1983 *J. Vac. Sci. Technol.* **1** 1137
- Sekiguchi H I, Sekiguchi T and Tananka K 1996 *Phys. Rev. B* **53** 12655
- [17] Takata Y, Edamatsu K, Yokoyama T, Seki K and Tohnan M 1989 *Japan. J. Appl. Phys.* **2** **28** L1282
- [18] Hoffman A, Petravac M, Comtet G, Heurtel A, Hellner L and Dujardin G 1999 *Phys. Rev. B* **59** 3203
- [19] Pate B B, Hecht M H, Binns C, Lindau I and Spicer W E 1982 *J. Vac. Sci. Technol.* **21** 364
- [20] Pate B B 1986 *Surf. Sci.* **165** 83
- [21] Knotek M L and Fiebelman P J 1978 *Phys. Rev. Lett.* **40** 964
- [22] Petravac M and Williams J S 1991 *Surf. Sci.* **259** 215
- [23] Hoffman A, Comtet G, Hellner L, Dujardin G and Petravac M 1998 *Appl. Phys. Lett.* **73** 1152
- [24] Hellner L, Philippe L, Dujardin G, Ramage M-J, Rose M, Cirkel P and Dumas P 1993 *Nucl. Instrum. Methods Phys. Res. B* **78** 342
- [25] Bandis C and Pate B B 1995 *Phys. Rev. B* **52** 12056
- [26] Comelli G, Stohr J, Robinson C J and Jark W 1988 *Phys. Rev. B* **38** 7511
- [27] Laikhtman A and Hoffman A 2002 *Diamond Relat. Mater.* **11** 371
- [28] Hoffman A, Laikhtman A, Comtet G, Hellner L and Dujardin G 2000 *Phys. Rev. B* **62** 8446
- [29] Laikhtman A, Gouzman I, Hoffman A, Dujardin G, Hellner L and Comtet G 1999 *J. Appl. Phys.* **86** 4192
- [30] Morar J F, Himpfel F J, Hollinger G, Jordon J L, Hughes G and McFeely F R 1986 *Phys. Rev. B* **33** 1346
- [31] Bobrov K, Comtet G, Dujardin G, Hellner L, Bergonzo P and Mer C 2001 *Phys. Rev. B* **63** 165421
- [32] Laikhtman A, Hoffman A, Kalish R, Breskin A and Chechik R 2000 *J. Appl. Phys.* **88** 2451
- [33] Krainsky I L and Asnin V M 1998 *Appl. Phys. Lett.* **72** 2574
- [34] Bobrov K, Shechter H, Folman M and Hoffman A 1999 *Diamond Relat. Mater.* **8** 705
- [35] Hoffman A, Praver S and Kalish R 1992 *Phys. Rev. B* **45** 12736
- [36] Diedrich L, Kuttel O M, Schaller E and Schlappbach L 1996 *Surf. Sci.* **349** 176
- [37] Asnin V M and Krainsky I L 1998 *Appl. Phys. Lett.* **73** 3727
- [38] Humphreys T P, Thomas R E, Malta D P, Posthill J B, Mantini M J, Rudder R A, Hudson G C, Markunas R J and Pettenkofer C 1997 *Appl. Phys. Lett.* **70** 1257
- [39] Hoffman A, Praver S and Kalish R 1992 *Diamond Relat. Mater.* **1** 440

- 
- [40] Hitchcock A P and Ishii I 1987 *J. Electron Spectrosc. Relat. Phenom.* **42** 11
- [41] Laikhtman A and Hoffman A 2003 *Surf. Sci.* **522** L1
- [42] Yeh J J and Lindau I 1985 *At. Data Nucl. Data Tables* **32** 1
- [43] Stohr J 1992 *NEXAFS Spectroscopy* (Berlin: Springer)
- [44] Graupner R, Maier F, Ristein J and Ley L 1998 *Phys. Rev. B* **57** 12397
- [45] Hossain M Z, Kubo T, Aruga T, Takagi N, Tsuno T, Fujimori N and Nishijima M 1999 *Japan. J. Appl. Phys.* **38** 6659
- [46] Hossain M Z, Kubo T, Aruga T, Takagi N, Tsuno T, Fujimori N and Nishijima M 1999 *Surf. Sci.* **436** 63
- [47] Pehrsson P E and Mercer T W 2000 *Surf. Sci.* **460** 49
- [48] Pehrsson P E, Mercer T W and Chaney J A 2002 *Surf. Sci.* **497** 13
- [49] Laikhtman A and Hoffman A 2002 *Phys. Status Solidi a* **193** 552